INVESTIGATING CHEMICAL PROPERTIES AND COMBUSTION CHARACTERISTICS OF TORREFIED MASSON PINE

Wanhe Hu
Master Candidate
E-mail: ZThuwanhe@163.com

Xiaomeng Yang
Doctor Candidate
E-mail:120003692@qq.com

Bingbing Mi
Master Candidate
E-mail:429543207@qq.com

Fang Liang
Master Candidate
E-mail:577759813@qq.com

Tao Zhang
Master Candidate
E-mail:1204624557@qq.com

Benhua Fei†
Professor
E-mail: feibenhua@icbr.ac.cn

Zehui Jiang†
Professor
E-mail: jiangzehui@icbr.ac.cn

*Zhijia Liu**
Doctor
International Centre for Bamboo and Rattan
Beijing, China, 100102
E-mail: Liuzj@icbr.ac.cn

(Received February 2016)

Abstract. To investigate chemical properties and combustion characteristics, masson pine was torrefied using a 1600× tube furnace in an argon atmosphere. The properties of torrefied masson pine were respectively determined through thermogravimetry, Fourier transform IR spectrometer, and X-ray diffraction. Results showed that thermal decomposition of hemicelluloses, cellulose, and lignin occurred during torrefaction processes. Crystalline region of cellulose was destroyed when temperature was up to 250°C. The effect of torrefaction temperature was more significant than that of residence time. Torrefaction

* Corresponding author
† SWST member

Wood and Fiber Science, 49(1), 2017, pp. 33-42

improved combustion characteristics of masson pine. The optimum process was 300°C of torrefaction temperature and 2.0 h of residence time. Combustion processing of torrefied masson pine included drying, oxidative pyrolysis, and char combustion. Torrefied masson pine had lower H/C and O/C ratios, peak temperature of oxidative pyrolysis and char combustion, and burnout temperatures. It had higher energy density, ignition temperature, and activation energy. These data will be significant to understand the torrefied masson pine for an energy product by direct combustion.

Keywords: Masson pine, combustion characteristic, TGA, FTIR, XRD.

INTRODUCTION

Biomass resources are considered as a type of renewable, sustainable, and clean energy feedstock, providing approximately 14% of the world's energy needs (Liu et al 2014b). For some developing countries, these resources provide about 35% of energy consumption (Hall et al 1992). Direct cofiring of biomass and coal is the simplest, cheapest, and most common way to use biomass for energy production in a coal-fired power plant. But the differences in physical and chemical properties of biomass materials create challenges when handling raw biomass for fuel or energy (Parikh et al 2007). There has been increased interest in the thermal pretreatment of biomass materials for combustion and cocombustion applications in recent years, such as steam explosion, pyrolysis, and torrefaction. Torrefaction is a feasible method to improve fuel properties of biomass. During this process, moisture present in the biomass is evaporated and the remaining components are pyrolyzed to gases including moisture (H_2O), carbon monoxide (CO), carbon dioxide (CO_2), and various organic acids. Torrefaction yields a solid uniform product with lower MC and higher energy content compared with those in the biomass feedstock. For example, the MC of bamboo decreased from 6.23% to 5.53% while the higher heating value increased from 18.52 to 27.09 kJ/g when bamboo was torrefied at temperature of 300°C and residence time of 2 h (Liu et al 2014b). Furthermore, completely torrefied biomass loses its original fiber structure, making it more suitable to be pulverized in coal mills. This benefit also enhances the biomass/coal ratio in power plants (Cremers 2009). Currently, torrefied biomass accounts for 15% of primary energy consumption worldwide (Chen and Kuo 2010; Seo et al 2010). It is considered as a main energy source for the future (Poudel and Oh 2014). For example, when corn stalks were torrefied in a horizontal tubular reactor at temperatures ranging from 150°C to 400°C and residence time varying from 0 to 50 min, the energy and mass yield were found to decrease with increasing temperature, whereas the high heating value (HHV) increased. Liu et al (2015) prepared biochars through the torrefaction processing with operating conditions at a specific temperature of 290°C and different residence times. They found that the calorific value of biochars correlated positively with its carbon contents with the maximum occurring at about 20 min. Bates and Ghoniem (2012) established a kinetics model for the evolution of the volatile and solid product combustion with torrefaction temperatures from 200°C to 300°C. They found that most of the volatiles were released in the first stage and included water, acetic acid, and carbon dioxide. In the second stage, the composition of the gases was mainly lactic acid, methanol, and acetic acid. Larsson et al (2013) investigated the effects of MC and torrefaction temperature on pilot scale pelletizing of torrefied Norway spruce. It was found that torrefaction temperature, residence times, and product characteristics were significant to the torrefaction process. Granados et al (2014) investigated the torrefaction process for six different types of residual biomass, including sugarcane bagasse, banana rachis, rice husk, palm oil fiber, sawdust, and coffee waste at temperature between 200°C and 300°C. They found that torrefaction was a way to transform the residual biomass and improve properties to use it in thermal processing. The most promising biomass was sawdust, which had an increase of 14.5% in HHV, from17.9 MJ/kg in its raw state to 20.5 MJ/kg after torrefaction.

Masson pine is one of the four types of typical fast-growing forestry plants in China, together with *Populus*, Chinese fir, and bamboo. Masson pine has been widely planted for its high economic value. The cultivated area of masson pine was about 2 million km^2 in 2012, about 13.2% of forest plantation in China. Furthermore, it has been used to produce wood-based panels, paper, and chemical products. These processes have produced abundant wastes of masson pine, which can be a great potential bioenergy resource in China. The previous research is very helpful in understanding fuel characteristics of wood, but masson pine is a different type of forestry resource. To the best of our knowledge, there is a lack of sufficient information concerning torrefied masson pine as a biomass fuel. Therefore, this research was carried out to investigate chemical properties and combustion characteristics of torrefied masson pine between temperatures of 200-300°C and 1.0-2.0 h of residence time. The chemical and structural transformations of torrefied masson pine were determined through Fourier transform IR spectrometer (FTIR) and X-ray diffraction (XRD). The combustion characteristics of torrefied masson pine were determined through thermogravimetric analysis (TGA). The results from this research will be very important and helpful to develop and utilize the waste of masson pine for energy products.

MATERIALS AND METHODS

Materials

Masson pine (*Pinus massoniana* Lamb.), aged 20 yr, was taken from Anhui Province, China. The MC of air-dried samples was about 9.5%. The samples were broken down to particles using a Wiley Mill. The materials were then screened to get particles between 250 and 425 μm. Before torrefaction, they were dried at a temperature of 105°C until the mass stabilized. Masson pine was torrefied at 200°C, 250°C, and 300°C for 1.0, 1.5, and 2.0 h, respectively, using a digitally controlled tube furnance. The torrefaction process was carried out in an argon environment. After torrefaction, the samples were immediately cooled in the desiccator to room temperature. Then the samples were transferred to separate Ziploc bags (Evergreen Plastics Mfg Co., Ltd) and sealed tightly.

Property Tests

FTIR test. The particles of torrefied masson pine were mixed with potassium bromide (KBr) in agate mortar. The mixing ratio was about 1:150. Then the mixture was pressed into pellets. Triplicate spectra of samples were collected by attenuated total reflectance using an 80-V FTIR spectrometer (Nexus 670, produced by Nicolet, America).

XRD test. XRD was used to understand the interaction of cellulose in lignocellulosic materials. Torrefied masson pine was treated using an X-ray diffractometer with an X-ray generator and a Cu target ($\lambda = 0.1540598$ nm) with Kα (40 kv, 40 mA) radiation at room temperature with the scan rate at 2.5°/min. Data were recorded each 0.02° (2θ) for the angle range of $2\theta = 5$–50°. The crystallinity index (CrI) was calculated according to formula (Zhang et al 2014):

$$\mathrm{CrI} = \frac{I_{002} - I_{\mathrm{am}}}{I_{002}} \quad (1)$$

where I_{002} is the overall intensity of the peak at 2θ about 22° and I_{am} is the intensity of the baseline at 2θ about 18°.

TGA test. Thermal decomposition was observed in terms of global mass loss though TGA Q 500 thermogravimetric analyzer (Produced by TA, America). First, the particles were evenly and loosely distributed in an open sample pan and the initial sample weight was about 3-6 mg. The temperature change was controlled from room temperature (30 ± 5°C) to 800°C with a heating rate of 20°/min. A high-purity nitrogen and air stream (flow rate of 60 mL/min) was continuously passed into the furnace. The experimental data could be directly obtained through the TGA Q 500 thermogravimetric

analyzer, but they were analyzed using origin 8.5 software.

Kinetics analysis. The fundamental rate equation used in all kinetics studies is generally described as:

$$\frac{d\alpha}{dt} = kf(\alpha) \quad (2)$$

where k is the rate constant and $f(\alpha)$ is the reaction model, a function depending on the actual reaction mechanism. Eq 2 expresses the rate of conversion, $d\alpha/dt$ at a constant temperature as a function of the reactant conversion loss and rate constant. In this study, the conversion rate α is defined as:

$$\alpha = \frac{(w_0 - w_t)}{(w_0 - w_f)} \quad (3)$$

where w_t, w_0, and w_f are time t, initial, and final weight of the sample, respectively. The rate constant k is generally given by the Arrhenius equation:

$$k = A\exp\left(\frac{-Ea}{RT}\right) \quad (4)$$

where Ea is the apparent activation energy (kJ/mol), R is the gas constant (8.314 J/K mol), A is the preexponential factor (min^{-1}), and T is the absolute temperature (K). The combination of Eqs 2 and 4 gives the following relationship:

$$\frac{d\alpha}{dt} = A\exp\left(\frac{-Ea}{RT}\right)f(\alpha) \quad (5)$$

For a dynamic TGA process, including the heating rate, $\beta = dT/dt$, into Eq 5, Eq 6 is obtained as:

$$\frac{d\alpha}{dT} = \left(\frac{A}{\beta}\right)\exp\left(\frac{-Ea}{RT}\right)f(\alpha) \quad (6)$$

Eqs 5 and 6 are the fundamental expressions of analytical methods to calculate kinetic parameters on the basis of TGA data.

Ultimate analysis. Ultimate analysis of torrefied masson pine was carried out according to standard methods. The determination of C, H, and N was performed according to GB/T 476-2008. The determination of S was performed according to GB/T 214-2007.

RESULTS AND DISCUSSION

The lignocellulosic biomass consists mainly of cellulose, hemicellulose, and lignin. The absorbance at 2923 cm^{-1} was a prominent carbon–hydrogen bond (C–H) stretching. There was a strong broad oxygen-carbon bond (O–H) stretching absorbance at 3429 cm^{-1}. In the fingerprint region (wavenumber from 750 to 2000 cm^{-1}), the peak at 804 cm^{-1} was attributed to C–H stretching and the peak at 895 cm^{-1} was attributed to glucose ring stretching, C–H deformation and C–H stretching out of plane of aromatic ring. The peak at 1030-1060 cm^{-1} was attributed to carbon–oxygen bond (C–O) stretching of polysaccharides of cellulose or hemicelluloses, the peak at 1110 cm^{-1} was attributed to hydroxyl association absorption band, the peak at 1158 cm^{-1} was stretching of carbon–oxygen–carbon bond (C–O–C) in cellulose and hemicelluloses. The peak at 1459 cm^{-1} was attributed to methylene (CH_2) blending; the peak at 1510 cm^{-1} was attributed to carbon–carbon double bond (C=C) stretching of aromatic compound from lignin; the peak at 1736 cm^{-1} was attributed to carbon–oxygen double bond (C=O) stretching vibration in lignin and hemicelluloses, and the peak at 1640 and 1750 cm^{-1} were attributed to C=O stretching vibration in hemicellulose (Sills and Gossett 2012; Chen et al 2014).

At 200°C torrefaction temperature, it can be seen in Fig 1 that the absorbance peaks with 1.0 h of residence time were similar with those of untreated masson pine except for the peaks at 1380 cm^{-1} (C–H bending of cellulose, hemicellulose, and lignin) and 1459 cm^{-1} (C–H deformation and asymmetric bending vibration of CH_3 and CH_2 groups from lignin). Compared with the spectra of 1.0 h of residence time, the peak at 895 cm^{-1} (glucose ring stretching, C–H deformation, C–H stretching out of the plane the of aromatic ring) was lost for 1.5 and 2.0 h of residence time, indicating thermal decomposition of glucose at 200°C. The peak at 1380 cm^{-1} decreased and

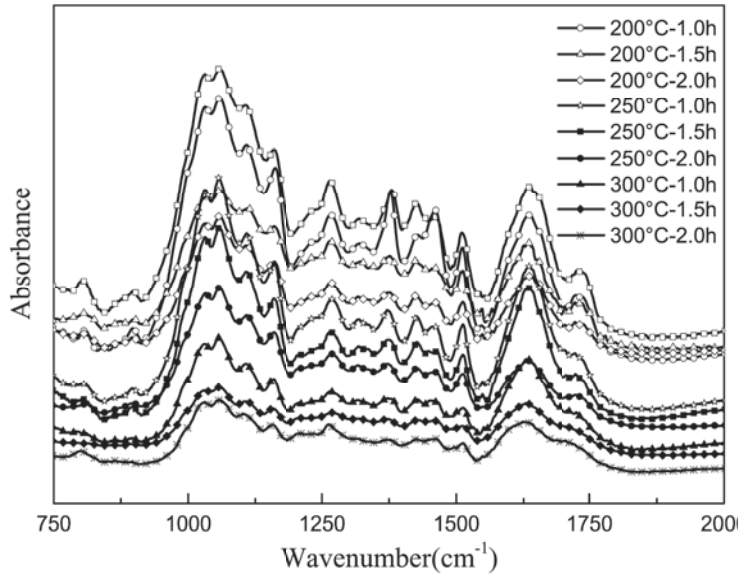

Figure 1. Fourier transform IR spectra of torrefied masson pine in finger region.

the peak at 1459 cm^{-1} slightly varied. The peaks at 1510 cm^{-1} (stretching of aromatic compound in lignin) and 1736 cm^{-1} (C=O stretching vibration in lignin and hemicelluloses) showed no change. However, when the temperature was up to 250°C, the peak at 1736 cm^{-1} obviously decreased but the peak change of 1158 (stretching in cellulose and hemicelluloses), 1425, 1510 cm^{-1} was insignificant. When the temperature was up to 300°C, the peaks at 895, 1380, 1459, and 1735 cm^{-1} disappeared. The FTIR result showed that cellulose, hemicellulose, and lignin underwent thermal decomposition during the torrefaction process according to the functional group change. The effect of torrefaction temperature was more significant than that of residence time. The thermal decomposition of cellulose, lignin, and hemicelluloses was a superposition. Hemicelluloses were the least thermally stable wood component. The thermal stability of lignin is greater than hemicelluloses and less than that of cellulose. Slopiecka et al (2012) found the thermal decomposition of hemicelluloses and cellulose took place in active pyrolysis with the temperature between 200°C and 380°C and 250°C and 380°C, respectively. Fierro et al (2005) confirmed that the decomposition of lignin started at about 200°C and did not complete until about 650°C.

Biomass materials exhibited two types of CrI, including absolute and relative CrI (Jiang et al 2012). The relative CrI was used in this research. The CrI of masson pine treated at different temperatures and times are shown in Table 1. It was found that the index of torrefied masson pine with 200°C and 250°C of torrefaction temperature were higher than that of untreated masson pine. The CrI of masson pine with 200°C and 250°C of torrefaction temperature were respectively 41.99%, 41.31%,

Table 1. The crystallinity index of torrefied masson pine.

Torrefaction process	Crystallinity index (%)
Control	40.96
200°C/1.0 h	41.99
200°C/1.5 h	41.31
200°C/2.0 h	41.31
250°C/1.0 h	43.55
250°C/1.5 h	41.74
250°C/2.0 h	42.48
300°C/1.0 h	36.08
300°C/1.5 h	29.91
300°C/2.0 h	23.59

41.31%, 43.55%, 41.74%, and 42.48%, compared with 40.96% of untreated masson pine. This indicated that the crystalline region of cellulose was not pyrolyzed, but absorbed water. Small molecules from hemicelluloses and amorphous regions of cellulose had been gradually degraded in the temperature scope. Liang and Xue (2014) reported that the hemicelluloses were entirely pyrolyzed with temperature from 200°C to 250°C, the cellulose was pyrolyzed with temperature from 240°C to 350°C, and the lignin was pyrolyzed from 280°C to 500°C. When chemical compositions of untreated masson pine were degraded except for the crystalline region of cellulose during the torrefaction process, its relative CrI gradually increased. It was also found that the CrI of torrefied masson pine with 300°C of torrefaction temperature was lower than that of untreated masson pine, indicating that cellulose pyrolysis moved from an amorphous region to a crystalline region. Shafizadeh (1984) indicated that cellulose decomposed on heating via two pathways. The first pathway dominated at temperatures below 300°C and it involved reduction in the degree of polymerization. The major decomposition products of this pathway were CO, CO_2, H_2O, and solid carbon-rich residue. The second pathway, which dominated at temperatures greater than 300°C, involved cleavage of molecules and disproportionation reactions to produce a mixture of anhydrous tar sugars and low molecular weight volatiles.

Figure 2 shows the changes in the atomic composition including hydrogen/carbon (H/C) and oxygen/carbon (O/C) ratios of torrefied masson pine. It was found that torrefied masson pine had lower H/C and O/C ratios, compared with untreated masson pine. This suggested the fuel qualities of torrefied masson pine were improved, reducing energy loss, smoke formation, and water vapor during the combustion process (Liu and Balasubramanian 2013). Table 2 shows that the C content of torrefied masson pine increases with increasing torrefaction temperature and residence time. Liu et al (2014a) found a good linear relationship between HHV of biomass fuel and its C content. Demirbas (1997) estimated HHV of biomass fuels according to a function of fixed carbon (HHV = 0.196 C content + 14.119). This indicated that the calorific value of torrefied masson pine had a higher HHV, compared with untreated masson pine. It was also confirmed that the H and O contents of torrefied masson pine were lower than that

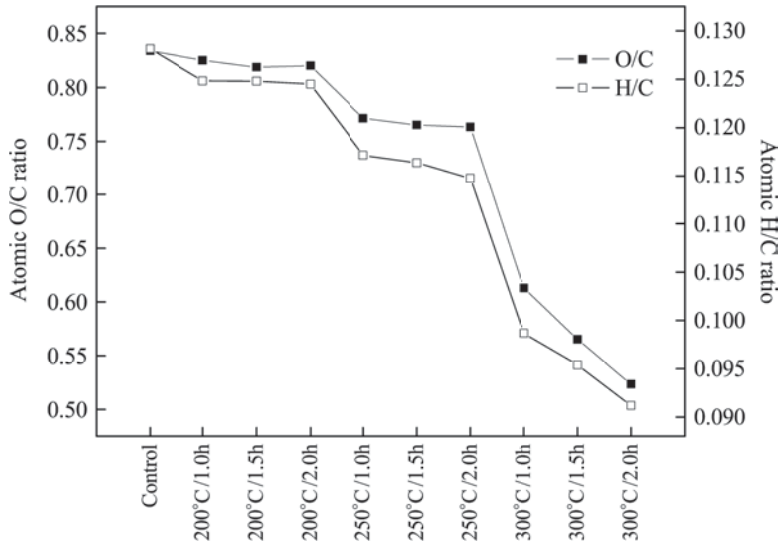

Figure 2. Atomic hydrogen/carbon and oxygen/carbon ratios of torrefied masson pine.

Table 2. Ultimate analyses and higher heat value of torrefied masson pine.

Ultimate analyses	Control	200°C/1.0 h	200°C/1.5 h	200°C/2.0 h	250°C/1.0 h	250°C/1.5 h	250°C/2.0 h	300°C/1.0 h	300°C/1.5 h	300°C/2.0 h
Carbon	50.95	51.27	51.44	51.41	52.93	53.11	53.24	58.38	60.17	61.85
Hydrogen	6.53	6.40	6.42	6.40	6.20	6.18	6.11	5.76	5.74	5.64
Oxygen (diff.)	42.50	42.31	42.12	42.17	40.83	40.64	40.64	35.79	34.01	32.39
Nitrogen	0.02	0.02	0.02	0.02	0.04	0.07	0.01	0.07	0.08	0.12
Sulfur	0.00	0.00	0.00	0.00	0.00	0.00	0.00	0.00	0.00	0.00
HHV	24.11	24.17	24.20	24.20	24.49	24.53	24.55	25.56	25.91	26.24

HHV, higher heating value.

of untreated masson pine. The pollutant emissions were affected by the sulfur and nitrogen contents in the biomass materials because of the formation of gaseous pollutants. Torrefied masson pine had a lower content of nitrogen compared with coal. It was interesting that masson pine did not have sulfur.

Figure 3 shows the combustion characteristics of torrefied masson pine with the airflow of 60 mL/min and the heating rate of 20°/min. There were three steps including drying, oxidative pyrolysis, and char combustion during the combustion process of torrefied masson pine. Table 3 shows combustion characteristics of torrefied masson pine from the TG curve. Untreated masson pine had a lower ignition temperature during the combustion process than that of torrefied masson pine. For torrefied masson pine, the ignition temperature increased with increase in torrefaction temperature and residence time. This was mainly attributed to thermal decomposition of chemical composition of masson pine during the torrefaction process. Volatile matters of masson pine were released at a lower temperature, which resulted in the more difficult ignition for torrefied masson pine. The peak temperature of oxidative pyrolysis and char combustion of torrefied masson pine shifted to lower temperature, indicating it had a better combustibility. Burnout temperature of torrefied masson pine also decreased even though the variation was

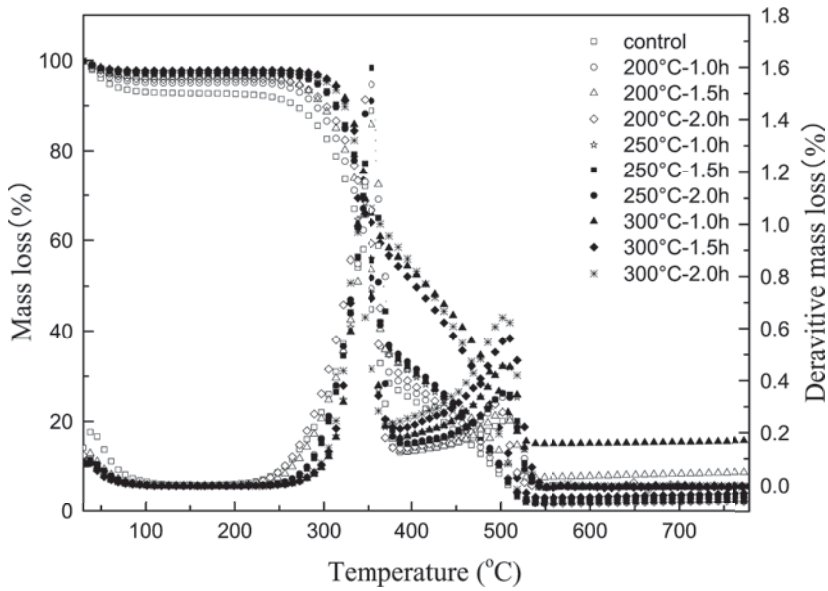

Figure 3. Combustion process of torrefied masson pine.

Table 3. Combustion characteristics of torrefied masson pine from thermogravimetric analysis.

		Oxidative pyrolysis			Char combustion			
Torrefaction process	T_i (°C)	T_p (°C)	DTG_{max} (mg/min)	W_1 (weight %)	T_p (°C)	DTG_{max} (mg/min)	W_1 (weight %)	T_b (°C)
Control	204	355	1.39	65.48	512	0.26	25.08	527
200°C/1.0 h	219	355	1.42	66.78	505	0.28	25.29	523
200°C/1.5 h	221	355	1.36	64.15	501	0.28	24.23	519
200°C/2.0 h	220	354	1.43	67.52	500	0.31	26.55	518
250°C/1.0 h	238	353	1.50	65.18	503	0.34	29.65	520
250°C/1.5 h	240	352	1.55	64.53	503	0.35	30.42	519
250°C/2.0 h	240	351	1.52	62.65	505	0.35	31.30	522
300°C/1.0 h	244	342	1.11	41.46	505	0.46	40.84	522
300°C/1.5 h	246	340	1.13	43.28	506	0.56	50.98	525
300°C/2.0 h	250	336	0.94	37.03	503	0.64	57.77	521

T_i, ignition temperature; T_p, peak temperature of this stage; W_l, weight loss of this stage; T_b, burnout temperature; TGA, thermogravimetric analysis.

not significant. The decrease in combustion temperature from ignition to burnout temperature indicated the combustion efficiency of torrefied masson pine was improved. The maximum rate of weight loss in the oxidative pyrolysis gradually increased when torrefaction temperature was up to 250°C, except for 200°C of torrefaction temperature and 1.5 h of residence time. There was a sudden decrease of the maximum rate of weight loss in the oxidative pyrolysis for 300°C of torrefaction temperature. In char combustion, the maximum rate of weight loss gradually increased with increase in torrefaction temperature and residence time. This was probably due to the higher fixed carbon content of torrefied masson pine, shown in Table 2. It was found that the maximum rate of weight loss in char combustion was obviously lower than that of oxidative pyrolysis. This indicated that there was a lower reactivity in char combustion, compared with oxidative pyrolysis.

Table 4 shows the kinetic parameters of torrefied masson pine, calculated by model-free methods (Liu et al 2012). The activation energy (*E*a) and exponential factor (*A*) were obtained according to the Arrhenius equation. Regression equations and the square of the correlation coefficient (R^2) were also presented in Table 4. The activation energy of untreated masson pine was 73.47 kJ/mol. The activation energy of torrefied masson pine increased in the range of 86.12-131.45 kJ/mol. This indicated torrefied masson pine would require higher temperatures and longer reaction times to oxidize compared with untreated masson pine. The reason is mainly due to thermal decomposition of masson pine during torrefaction process (El-sayed and Mostafa 2015; Titirici and Antonietti 2009).

Table 4. Thermal kinetics for torrefied masson pine.

Torrefaction process	Linear function	Correlation coefficient value ($R^{2)}$	*E*a (kJ/mol)	*A* (1/min)
Control	$y = -8{,}837x + 0.9427$	0.971	73.47	$4.54E+05$
200°C/1.0 h	$y = -10{,}359x + 3.2897$	0.986	86.12	$5.56E+06$
200°C/1.5 h	$y = -11{,}025x + 4.3344$	0.996	91.66	$1.68E+07$
200°C/2.0 h	$y = -10{,}690x + 3.7551$	0.988	88.88	$9.14E+06$
250°C/1.0 h	$y = -14{,}366x + 9.5192$	0.997	119.44	$3.91E+09$
250°C/1.5 h	$y = -13{,}765x + 8.5567$	0.997	114.44	$1.43E+09$
250°C/2.0 h	$y = -14{,}563x + 9.8003$	0.996	121.08	$5.25E+09$
300°C/1.0 h	$y = -13{,}988x + 8.4085$	0.912	116.30	$1.25E+09$
300°C/1.5 h	$y = -15{,}811x + 11.494$	0.954	131.45	$3.10E+10$
300°C/2.0 h	$y = -13{,}653x + 7.9785$	0.945	113.51	$7.97E+08$

*E*a, activation energy; *A*, exponential factor.

CONCLUSIONS

The thermal decomposition of hemicelluloses, cellulose, and lignin occurred during the torrefaction process. The crystalline region of cellulose was destroyed when temperature was up to 250°C. The effect of torrefaction temperature was more significant than that of residence time. Torrefaction improved combustion characteristics of masson pine. The optimum process was 300°C of torrefaction temperature and 2.0 h of residence time. The combustion processing of torrefied masson pine included drying, oxidative pyrolysis, and char combustion. There was a lower reactivity in char combustion, compared with oxidative pyrolysis. Torrefied masson pine had lower H/C and O/C ratios, peak temperature of oxidative pyrolysis and char combustion, and burnout temperature. It had a higher energy density, ignition temperature, and activation energy. Torrefied masson pine reduced energy loss, smoke formation, and water vapor during the combustion process. It also had a more steady-state burning process and a higher combustion efficiency.

ACKNOWLEDGMENTS

This research was financially supported by Basic Scientific Research Funds of the International Centre for Bamboo and Rattan (co-firing technology of torrefied bamboo and coal).

REFERENCES

Bates RB, Ghoniem AF (2012) Biomass torrefaction: Modeling of volatile and solid product evolution kinetics. Biores Technol 124:460-469.

Chen WH, Kuo PC (2010) A study on torrefaction of various biomass materials and its impact on lignocellulosic structure simulated by a thermogravimetry. Energy 35:2580-2586.

Chen CJ, Luo JJ, Qin W, Tong ZF (2014) Elemental analysis, chemical composition, cellulose crystallinity, and FTIR spectra of *Toona sinesis* wood. Monatsh Chem 145:175-185.

Jaap K, Shahab S, Staffan M, Sebnem M (2012) Status overview of torrefaction technologies. IEA Bioenergy Task 32, 1-54.

Demirbas A (1997) Calculation of higher heating values of biomass fuels. Fuel 76:431-434.

El-sayed SA, Mostafa MA (2015) Kinetic parameters determination of biomass pyrolysis fuels using TGA and DTA techniques. Waste Biomass Valor 6:401-415.

Fierro V, Torné-Fernández V, Montané D, Celzard A (2005) Study of the decomposition of kraft lignin impregnated with orthophosphoric acid. Thermochim Acta 433:142-148.

Granados DA, Velásquez HI, Chnjne F (2014) Energetic and exergetic evaluation of residual biomass in a torrefaction process. Energy 74:181-189.

GB/T 214-2007. Determination of total sulfur in coal, analysis standard of China. D21 75.160.10.

GB/T 476-2008. Determination of carbon and hydrogen in coal, analysis standard of China. D21 73.040.

Hall DO, Rosillo-Calle F, de Groot P (1992) Biomass energy lessons from case studies in developing countries. Energy Policy 1:62-73.

Jiang HZ, Liu ZJ, Fei BH, Cai ZY, Yu Y, Liu XE (2012) The pyrolysis characteristics of moso bamboo. J Anal Appl Pyrolysis 94:48-52.

Larsson SH, Rudolfsson M, Nordwaeger M, Olofsson I, Samulesson R (2013) Effects of moisture content, torrefaction temperature and die temperature in pilot scale pelletizing of torrefied Norway spruce. Appl Energy 102:827-832.

Liang FY, Xue ZH (2014) The low temperature pyrolysis characteristics of Salix. Wood Processing Machinery 4:48-52.

Liu ZG, Balasubramanian R (2013) A comparison of thermal behaviors of raw biomass, pyrolysis biochar and their blends with lignite. Biores Technol 146: 371-378.

Liu ZJ, Fei BH, Jiang ZH, Liu XE (2014a) Combustion characteristics of bamboo-biochars. Biores Technol 167: 94-99.

Liu ZJ, Jiang ZH, Fei BH, Cai ZY, Liu XE (2014b) Comparative properties of bamboo and pine pellets. Wood Fiber Sci 46:510-518.

Liu SC, Tsai WT, Li MH, Tsai CH (2015) Effect of holding time on fuel properties of biochars prepared from torrefaction of coffee residue. Biomass Convers Biorefin 5:209-214.

Liu ZG, Quek A, Hoekman SK, Srinivasan MP, Balasubramanian R (2012) Thermogravimetric investigation of hydrochar-lignite co-combustion. Biores Technol 123:646-652.

Parikh J, Channiwalab SA, Ghosal GK (2007) A correlation for calculating elemental composition from proximate analysis of biomass materials. Fuel 86: 1710-1719.

Poudel J, Oh SC (2014) Effect of torrefaction on the properties of corn stalk to enhance solid fuel qualities. Energy 7:5586-5600.

Seo DK, Park SS, Hwang JYT (2010) Study of the pyrolysis of biomass using thermo-gravimetric analysis (TGA) and concentration measurements of the evolved species. J Anal Appl Pyrolysis 89:66-73.

Shafizadeh F (1984) The chemistry of solid wood. American Chemical Society, Washington, DC, pp. 489-529.

Sills DL, Gossett JM (2012) Using FTIR to predict saccharification from enzymatic hydrolysis alkali-pretreated biomass. Biotechnol Bioeng 109:353-362.

Slopiecka K, Bartocci P, Fantozzi F (2012) Thermogravimetric analysis and kinetic study of poplar wood. Appl Energy 97:491-497.

Titirici MM, Antonietti M (2009) Chemistry and materials options of sustainable carbon materials made by hydrothermal carbonization. Chem Soc Rev 39: 103-116.

Zhang JF, Wang YX, Zhang LY, Liu GQ, Cheng G (2014) Understanding changes in cellulose crystalline structure of lignocellulose biomass during ionic liquid pretreatment by XRD. Biores Technol 151:402-405.